

# Computational Study of Benzene-to-Phenol Oxidation Catalyzed by N<sub>2</sub>O on Iron-Exchanged Ferrierite

Nelly A. Kachurovskaya,<sup>\*,†</sup> Georgii M. Zhidomirov,<sup>‡</sup> and Rutger A. van Santen<sup>†</sup>

Schuit Institute of Catalysis, Laboratory of Inorganic Chemistry and Catalysis, Eindhoven University of Technology, P.O. Box 513, 5600MB, Eindhoven, The Netherlands, and Boreskov Institute of Catalysis, Pr. Lavrentieva 5, Novosibirsk 630090, Russia

Received: February 27, 2003; In Final Form: October 31, 2003

An Fe(II) ion at an  $\alpha$ -cation exchange position of ferrierite, (Fe) $_{\alpha}$ , was taken as a model for the active site in nitrous oxide decomposition and in the selective oxidation of phenol with nitrous oxide. The oxygen that is deposited via the decomposition of N<sub>2</sub>O is commonly referred to as  $\alpha$ -oxygen, (O) $_{\alpha}$ . Comparison with the results of cluster model calculations was performed for reaction of benzene-to-phenol oxidation. Periodic calculations predict the same reaction path for benzene oxidation as does the cluster model study. Differences in the adsorption modes for both types of calculations were analyzed and discussed.

## Introduction

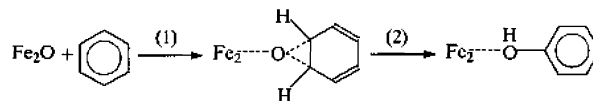
Zeolites are useful catalysts for the selective oxidation of hydrocarbons with nitrous oxide, especially for the direct process of benzene-to-phenol oxidation.<sup>1,2</sup> Thermodynamically, N<sub>2</sub>O is an unstable endothermic molecule ( $\Delta H_f^\circ = +19.5$  kcal/mol); however, kinetically, it is quite stable. Its noncatalytic decomposition becomes noticeable only above 600 °C.

In 1983, Iwamoto et al. were the first to use N<sub>2</sub>O for the oxidation of benzene to phenol.<sup>3</sup> This reaction lead to a better selectivity, compared to that of oxidation by dioxygen. At 550 °C, the reaction selectivity with a vanadia catalyst exceeded 70%. These results stimulated further efforts to search for new, more-effective catalytic systems. A few groups discovered independently that iron-incorporated ZSM-5 zeolites are the best catalysts for this reaction.<sup>1,2,4</sup> Such catalysis allowed for the reaction to proceed at a much lower temperature and, more importantly, with selectivity approaching 100%. The discovery of the selective zeolite catalysts for oxidation reactions is rather unique, and it raises several fundamental questions.

In regard to the location of the Fe ion, Fe ions can, in principle, occupy three positions in the zeolite matrix: (i) isolated ions in the tetrahedral lattice positions (substituting silicon), (ii) isolated ions or small complexes inside the channels, or (iii) dispersed oxide particles on the outer surface of the zeolite. Several studies have been conducted to determine which of these positions coincide with the commonly referred  $\alpha$ -sites.<sup>5,6</sup> Experimental results exclude the first and third possibilities. Thus,  $\alpha$ -sites should be inside the channel of the zeolite matrix. A model for these sites is presented at the beginning of the Results and Discussion section. It is important to note that the amount of introduced iron should be <0.1 wt % Fe<sub>2</sub>O<sub>3</sub>; for the optimal activity of Fe-ZSM-5 in benzene-to-phenol oxidation with nitrous oxide, the maximum concentration of  $\alpha$ -sites could be determined to be 10<sup>19</sup>–10<sup>20</sup> sites/g.<sup>7</sup> Iron can be introduced in the system via different procedures.<sup>8</sup> The most favorable way

is to introduce it during synthesis.<sup>9,10</sup> High-temperature calcination and steaming treatment is necessary to increase the concentration of  $\alpha$ -sites.<sup>11</sup> During such a treatment, practically all iron migrates from lattice framework positions toward extra framework positions.<sup>12</sup> After such a treatment, a significant portion of the Fe cations appear to be in the divalent (Fe<sup>2+</sup>) state.<sup>13</sup> Fe<sup>2+</sup> cations in  $\alpha$ -sites can be easily oxidized to the trivalent state (Fe<sup>3+</sup>) through the decomposition of N<sub>2</sub>O with formation of monatomic  $\alpha$ -oxygen (O) $_{\alpha}$ .

A correlation between the concentration of  $\alpha$ -oxygen and that of reduced Fe<sup>2+</sup> forms was observed.<sup>9,13</sup> The reduced Fe<sup>2+</sup> state cannot be oxidized by molecular oxygen, even at a rather high temperature. The subject of the nuclearity of  $\alpha$ -sites has been extensively debated.<sup>14</sup> Significant evidence has been given that the  $\alpha$ -sites are monatomic and in a paired arrangement as in binuclear complexes.<sup>9</sup> Each of the Fe ions in the binuclear structure is capable of generating (O) $_{\alpha}$  independently. These  $\alpha$ -oxygens could produce very selective oxidation of hydrocarbons, for example, the oxidations of benzene to phenol and methane to methyl alcohol under ambient conditions. The high reaction rates assume the one-step direct insertion of (O) $_{\alpha}$  in the C–H bond of hydrocarbons. This is in agreement with the observation of the important kinetic H/D isotope effect (KIE) in the methane oxidation: KIE  $\approx$  3.2 at a temperature of  $T = 25$  °C.<sup>15</sup> Contrary to the case of methane, no KIE in benzene oxidation by (O) $_{\alpha}$  was observed. Based on these experimental data, a mechanism was proposed for benzene oxidation by  $\alpha$ -oxygen, which is illustrated by the following scheme:<sup>15</sup>



where (1) was supposed to be a rate-limiting step.

The first theoretical study of the reaction path for benzene-to-phenol oxidation reaction from  $\alpha$ -oxygen has been published in ref 16. A traditional 3T cluster structure was chosen to model the cationic position of Fe<sup>1+</sup>, and a two-step mechanism of benzene oxidation with intermediate breaking of the C–H bond was considered. Although the calculations of intermediates and

\* Author to whom correspondence should be addressed. E-mail address: N.A.Kachurovskaya@tue.nl.

<sup>†</sup> Eindhoven University of Technology.

<sup>‡</sup> Boreskov Institute of Catalysis.

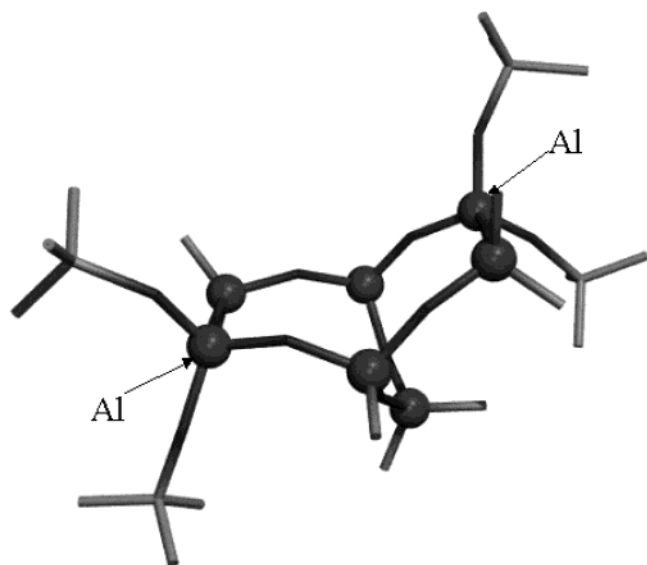
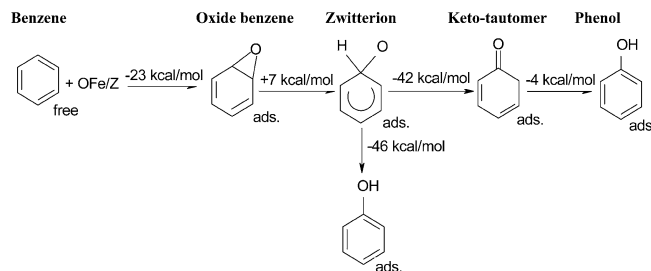


**Figure 1.** Initial model for cluster calculations (crystallographic  $\alpha$ -position).

**SCHEME 1: Reaction Path of Benzene-to-Phenol Oxidation, According to Previous Study<sup>17</sup>**



transition states were quite reasonable, the choice for Fe<sup>1+</sup> in the model of the  $\alpha$ -site seems to be rather questionable. Also, the reaction mechanism proposed does not agree with the experimental data on the kinetic isotope effect measurements. In ref 17, we have performed cluster model DFT calculations to study the mechanism of benzene-to-phenol oxidation by N<sub>2</sub>O on FeZSM-5 zeolite. The  $\alpha$ -cationic position presented in Figure 1 was chosen for the location of Fe<sup>2+</sup>, according to ref 18, which was an effective six-membered ring with two Al atoms on the wall of the straight channel of the zeolite. Such a model of Fe<sup>2+</sup> stabilization in Fe-ferrierites with Fe/Al < 0.1 was discussed recently in ref 19. For the two nearest  $\alpha$ -cationic positions, the Fe–Fe distance between two Fe ions is 5.4 Å, which can explain, in principle, the paired Fe arrangement observation.<sup>9</sup> At the same time, each of the single centers of such a paired arrangement can react with N<sub>2</sub>O separately,<sup>9</sup> and it was the basic assumption of our study.<sup>17</sup> The mechanism of this reaction has been defined more precisely according to Scheme 1.

The ease of the benzene oxide formation during the adsorption of benzene on the oxygen-containing  $\alpha$ -center led to the conclusion that step (1) is not rate-limiting. This is contrary to the Panov et al. proposition. In ref 17, it was shown that the transfer of the benzene oxide to the next intermediate by breaking one of the two C–O bonds is the rate-limiting step. The transformation of the intermediate to the keto-tautomer and phenol are the following steps. This reaction path is quantitatively the same as that previously suggested for acidic catalysis transformations of benzene oxide to phenol in solution.<sup>20,21</sup>

Cluster models present some limitations in calculations of the chemical reaction pathways on heterogeneous catalysts. The

correct description of the zeolite lattice flexibility near the adsorption center and a proper account of the crystalline environment and cavity shape and size are the most important ones. When the geometry is optimized, special constraints must be used for the cluster model calculations of the reaction pathways.<sup>22,23</sup> This can help to solve the problem of the adsorption center flexibility. However, these constraints can be used in different ways, and they introduce some uncertainty.<sup>24</sup> Information on the influence of the zeolite can be obtained by embedding of the quantum chemical cluster in a classical potential that describes the interactions with the zeolite framework. The force field used in the molecular mechanics portion and the method for coupling of the quantum chemical and the molecular mechanics determine partially the quality of this method. Quantum-chemical periodic structure calculations have the advantage of not requiring such embedding approaches and allow for a more natural description of the flexibility of the lattice.

It is necessary to mention that it was widely believed that computations including transition-metal elements or oxygen would be completely intractable with pseudopotentials in a plane-wave representation.<sup>25</sup> However, several studies have shown that pseudopotential calculations can be performed for systems containing these atoms through the use of a substantial but manageable number of plane-waves in the basis set.<sup>26–30</sup> This method was successfully used to study the stability of Zn<sup>2+</sup> cations in zeolites.<sup>31</sup> However, we are the first to use this approach to calculate the reaction mechanism catalyzed by zeolites with incorporated transition metals. One of the purposes of this study is to check the possibility of using pseudopotentials in a plane-wave representation for calculations of the reaction mechanisms of oxide systems with incorporated transition metals.

Thus, in this work, we present a periodic density functional theory (DFT) study of the mechanism of benzene-to-phenol oxidation by N<sub>2</sub>O. The  $\alpha$ -cationic position of ferrierite is chosen as the initial model for calculation. We chose the ferrierite lattice because its smaller unit cell makes calculations less demanding. This position is similar to the  $\alpha$ -position in ZSM-5 zeolite. A comparison with cluster model calculations performed in ref 17 allowed us to analyze effect of the zeolite lattice and consequential spatial constraints on the reaction pathway.

### Computational Details

Periodic ab initio calculations have been performed, using the Vienna Ab Initio Simulation Package (VASP).<sup>25</sup> With VASP codes, periodic pseudopotential density functional calculations are conducted in a plane-wave basis set. The exchange-correlation functional of the generalized gradient approximation (GGA) of Perdew and Wang<sup>26</sup> is used in the DFT calculations.

The interaction between the atomic core and electrons is described using the ultrasoft pseudopotentials (US–PP) that have been introduced by Vanderbilt<sup>27</sup> and developed by Kresse and Hafner.<sup>28</sup> These pseudopotentials allow a drastic reduction of the number of the plane waves per atom used in the basis. The recommended cutoff for the plane wave basis for first-row elements is 300–400 eV, where a value of 370–400 eV is required to predict vibrational properties accurately; however, binding geometries and energy differences are usually well-reproduced with 325 eV. The typical errors in bond length for oxygen dimers (O<sub>2</sub>, CO) with this cutoff are ~1%, compared to more accurate DFT calculations.<sup>32</sup> The cutoff value of 300 eV was successfully used for the theoretical study of the alkylation reaction of toluene with methanol catalyzed by acidic

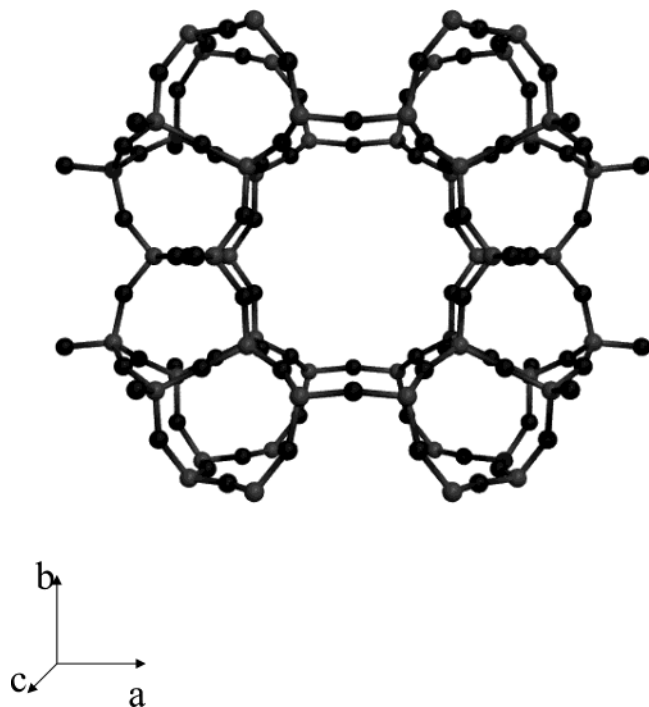


Figure 2. Ferrierite unit cell.

mordenite.<sup>35</sup> For these reasons, a cutoff value of 325.0 eV has been used in our calculations. Parameters, such as the k-point, were kept fixed and equal to one (the  $\Gamma$ -point version of VASP). The  $\alpha$ -position in ferrierite is similar to that in ZSM-5 zeolite. It contains 36  $\text{TO}_2$  units per unit cell, which is substantially less than that in ZSM-5 zeolite. The original model consists of one unit cell of ferrierite (orthorhombic cell,  $a = 19.156$ ,  $b = 14.127$ ,  $c = 7.489$ ) (see Figure 2). This unit cell is optimized at a constant volume, using a quasi-Newton algorithm that is based on the minimization of analytical forces. Convergence is assumed when forces acting on the unit-cell atoms are  $<0.05$  eV/Å. To correct for the inadequacy of the van der Waals interaction prediction, we perform calculations of the benzene molecule in the cavity of the zeolite matrix.

In the case of a drastic disagreement with the cluster model study, which happen for the adsorption complexes of phenol molecules, additional calculations are performed using projected augmented-wave (PAW) method. Radial cutoffs (core radii) are smaller in PAW than those used for the US-PP. The PAW potentials reconstruct the exact valence wave function with all nodes in the core region. There are several instances where the PAW method has distinctive advantages over US-PP. In particular, for transition metals with a large magnetic moment, very accurate results are difficult to obtain with the US-PP approach.<sup>36,37</sup> For some elements, several PAW versions exist. For Fe ions,  $\text{Fe}_{-pv}$  PAW potential is used. This implies that the 3p semi-core states are treated as valence states. For Si, Al, C, and H atoms, standard version of PAW pseudopotentials are used.

## Results and Discussion

**Model of “ $\alpha$ -center”.** To model the “ $\alpha$ -center”, two Al atoms were placed into the ferrierite framework, substituting two distant framework Si atoms within the same unit cell. The  $\text{Fe}^{2+}$  atom was placed in the middle of the  $\alpha$ -position.  $\text{Fe}^{2+}$  particles are paramagnetic; therefore, spin-polarized calculations were performed with a total spin equal to 2. The optimized iron-containing structure is shown in Figure 3. The cation is stabilized

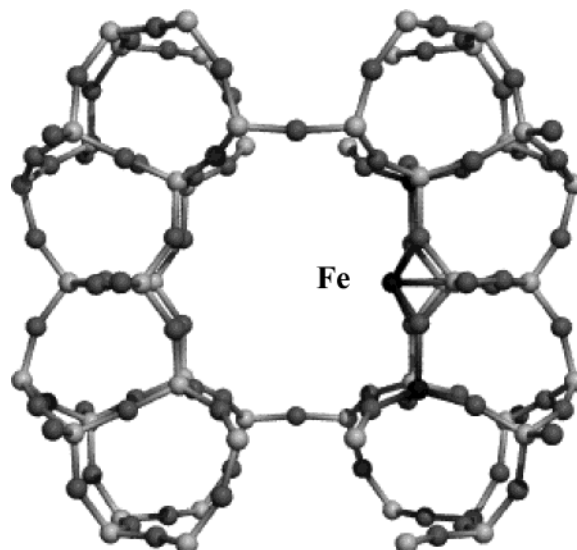


Figure 3. Optimized structure of the  $\text{Fe}^{2+}$  cation in  $\alpha$ -cationic exchange position.

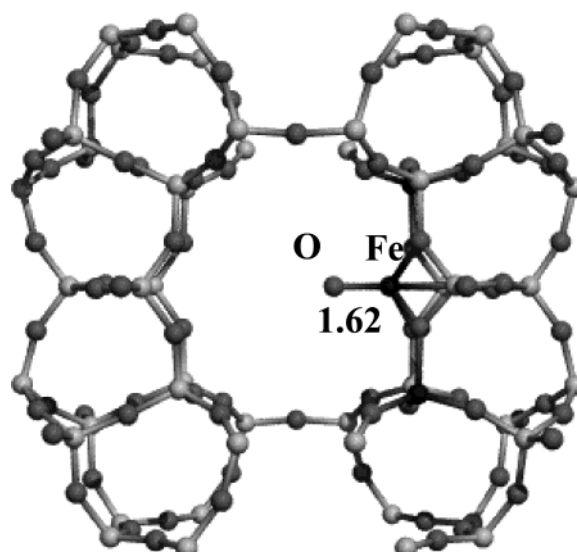
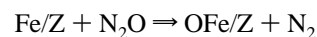


Figure 4. Structure of  $\alpha$ -oxygen species.

by the interaction with four O ions of the effective six-membered ring in the  $\alpha$ -cationic position. Comparison with the analogous cluster model structures<sup>17</sup> reveals differences in the Fe coordination. In the cluster model calculations, the adsorption of iron results in an essential deformation of the adsorption center structure, which causes coordination of the Fe atom with four O atoms, bonded to Al ions. In the case of periodic calculations, the Fe atom coordinates with two O atoms bound to Al ions and two O atoms bound to only Si ions. The bond distances  $R(\text{Fe}-\text{O}_{\text{Si}})$  and  $R(\text{Fe}-\text{O}_{\text{Al}})$  are 2.16 and 2.02 Å, respectively.

Next, a surface oxygen species modeling the  $\alpha$ -oxygen responsible for the catalytic reactivity of ion-exchanged Fe zeolites are studied. The structure of  $\alpha$ -oxygen is presented in Figure 4. This center is formed by  $\text{N}_2\text{O}$  decomposition on a  $(\text{Fe})_\alpha$  site, according to the reaction



The reaction is exothermic, with a heat of reaction equal to  $-14.7$  kcal/mol. The calculated  $\text{Fe}=\text{O}$  bond length is 1.62 Å for periodic calculations and 1.59 Å for the cluster model.<sup>17</sup> The  $\text{Fe}=\text{O}$  bond energy is calculated by evaluating the reaction



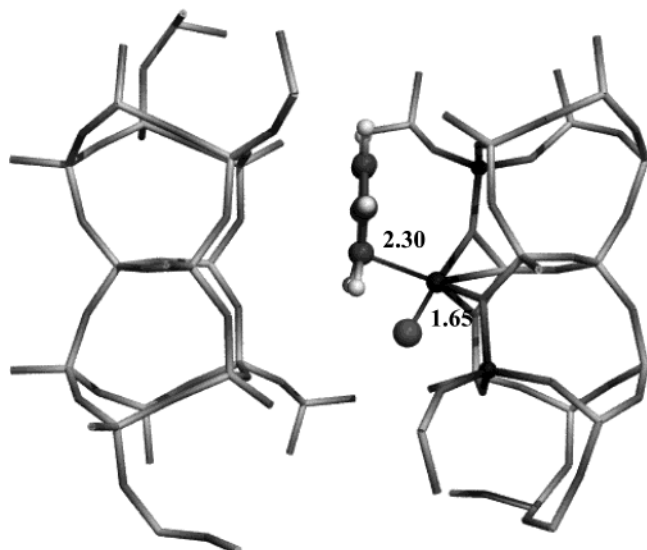
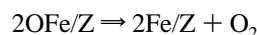


**Figure 5.** Adsorption complex of the benzene molecule on the active site.

energy for the reaction



which is  $\sim 70$  kcal/mol for the periodic calculations and 55.5 kcal/mol for the cluster calculations. This is in reasonable agreement with the value obtained from calorimetric measurements ( $60 \pm 10$  kcal/mol).<sup>38</sup>

**Reaction Path.** We concentrate the discussion of the periodic structure calculations on the adsorption of intermediates formed in the reaction path.

We start by performing fixed-point calculations. The benzene molecule has been placed in the cavity of ferrierite and a geometry optimization has been performed, which enables us to compute the energy profile without explicitly calculating van der Waals interactions, using approximate expressions. A free benzene molecule also has been optimized. The computed sum of the free benzene molecule and the FeO/ferrierite structure energies is more stable than the structure with the benzene molecule located in the cavity of zeolite (by 8.7 kcal/mol). The experimentally measured heat of sorption of the benzene molecule in H-ZSM-5 is dependent on the sorbate loading and is  $\sim 12.2$  kcal/mol.<sup>39</sup> Thus, the van der Waals correction to the calculated benzene–zeolite guest–host system energy is 20.9 kcal/mol.

To study the catalytic mechanism, we tried to find an adsorption complex of the benzene molecule with an  $\alpha$ -center, OFe/Z. The optimized structure of this complex corresponds to bonding of the benzene ring with an Fe atom and it is shown in Figure 5. The adsorption energy of the complex is 14 kcal/mol. In the cluster calculations,<sup>17</sup> no adsorption of the benzene molecule has been observed.

Geometry optimizations of the benzene oxide and oxepin molecules have been performed, following the reaction mechanism proposed in ref 17. Interesting results are obtained for the adsorption complexes of intermediates. An adsorption complex of the benzene oxide molecule has been observed. It is a bifurcated adsorption mode through the O atom and  $\pi$ -system. The structure of the latter is shown in Figure 6. The bond lengths  $R(\text{Fe}–\text{O})$  and  $R(\text{Fe}–\text{C})$  are 2.27 and 2.36 Å, respectively. They can be considered to be weak coordination bonds. Under the influence of the adsorption, the structure of the adsorption center is destroyed. The Fe atom moves from

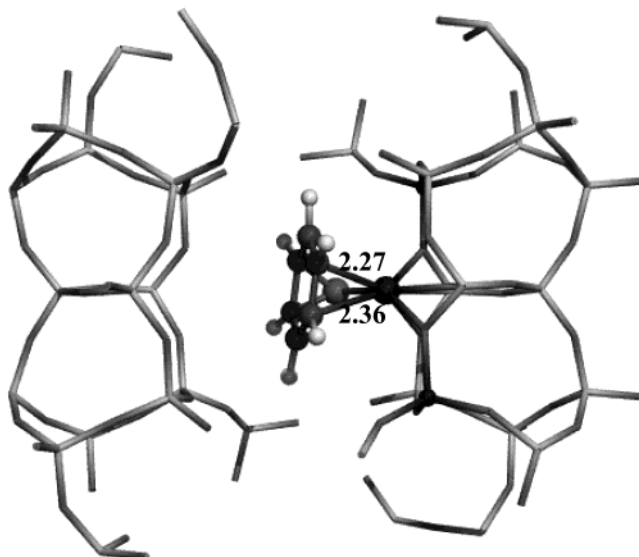


**Figure 6.** Optimized structure of the adsorbed benzene oxide molecule.

**TABLE 1: Energetic Effects of the Transformations, Compared to the Benzene Molecule Adsorbed in the Cavity of Ferrierite**

structure	$\Delta E$ (kcal/mol)
benzene in cavity	0.0
adsorbed benzene molecule	−14
benzene oxide	−28
oxepin (see Figure 6a)	+38
oxepin (see Figure 6b)	−11
oxepin (see Figure 6c)	−28
zwitterion intermediate	−19
keto-tautomer	−42
phenol (see Figure 9a)	−75
phenol (see Figure 9b)	−66
phenol (see Figure 9c)	−15

the center of the ferrierite  $\alpha$ -position and it loses its connection with one O atom from the Si–O–Si lattice fragment. Similar distortions have been observed for all adsorption complexes. In this adsorption structure, Fe is connected to two O atoms from Al–O–Si fragments, with bond distances of 2.10 Å, and there is a bond with the O atom from Si–O–Si fragments, with  $R(\text{Fe}–\text{O}_{\text{Al}}) = 2.15$  Å. This adsorption mode differs from that of the cluster model calculations where only adsorption with benzene oxide via the O atom occurs. Although structures of adsorption complexes differ for cluster and periodic calculations, the corresponding formation energies of the benzene oxide molecule are quite the same. They are approximately  $-26$  kcal/mol for the periodic and  $-23$  kcal/mol for the cluster calculations. Energetic effects of the transformations are summarized in Table 1.

The interpretation of the results after geometry optimization is not trivial. There are many local minima on the potential surface and, depending on the choice of the initial structure, different adsorption complexes can be found. Confidence never exists whether the global minimum is found; only chemical knowledge about some intermediates can help to elucidate the reaction pathway. The potential surface in the cavity of ferrierite seems to be very flat. We have performed calculations for the adsorption complexes with the initial orientation in the different crystallographic planes of ferrierite. Structures of the adsorption complexes are quite the same, and the differences in adsorption energies that were observed are on the order of a few kilocalories per mole. Our conclusion is that this cannot influence the interpretation of the reaction mechanism.

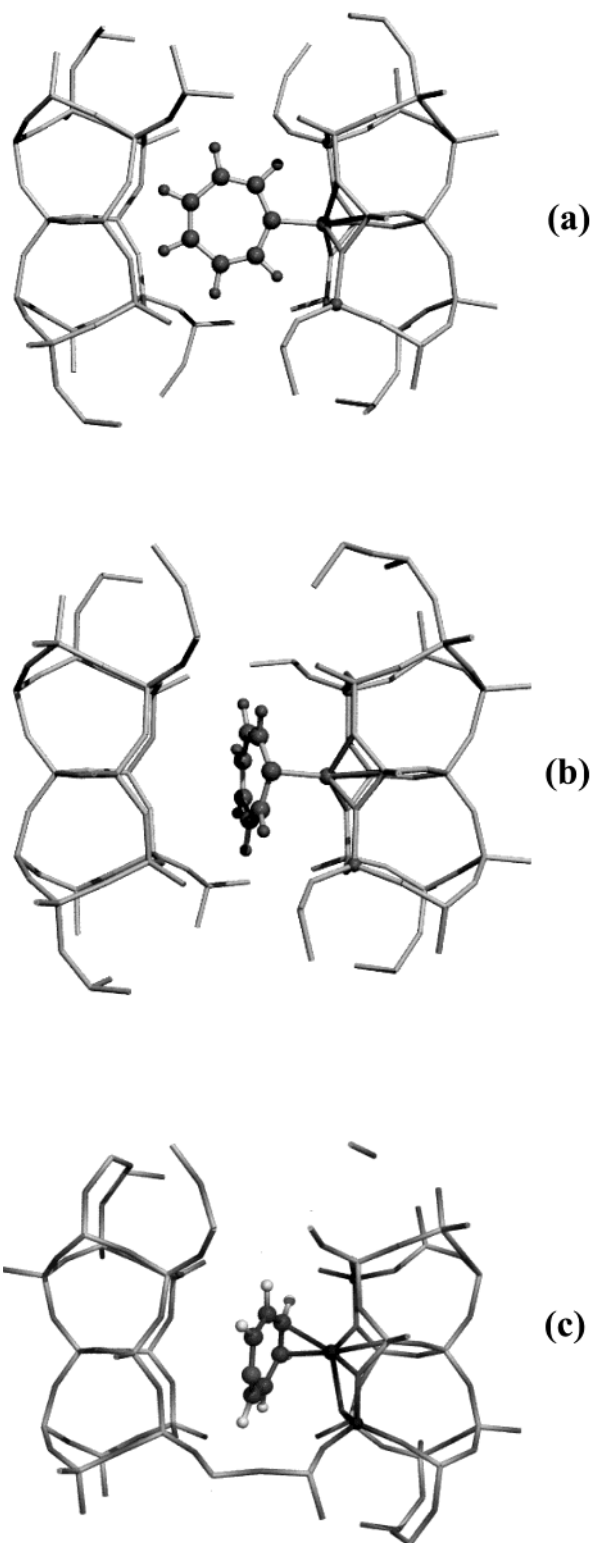


**Figure 7.** Optimized structures of the oxepin molecule in the cavity of ferrierite.

For the tautomer of the benzene oxide molecule, the so-called oxepin, three optimized structures have been found. Oxepin is a seven-member ring formed by six C atoms and one O atom. Two adsorbed structures are adsorption complexes formed via the O atom (see Figure 7a and b). The third one corresponds to the adsorption via the  $\pi$ -system (see Figure 7c). The  $\pi$ -adsorption complex has been located using the molecular dynamics approach, and, after that, its structure has been optimized according to the technique described in the Computational

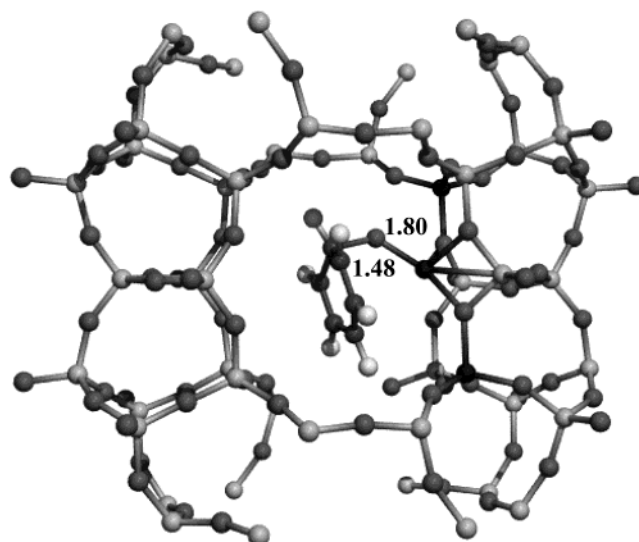


**Figure 8.** Structure of the adsorbed zwitterions intermediate on the active site.

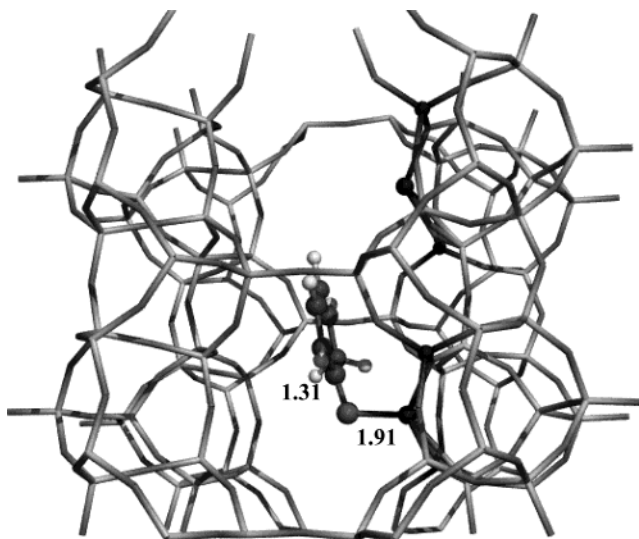


**Figure 9.** Optimized structure of the keto-tautomer of phenol molecule in the adsorption state.

Details section. Adsorption by the  $\pi$ -system of the oxepin molecule is preferred by 17 kcal/mol, in comparison to the more-stable (Figure 7b) adsorption on the O atom. The bond distance  $R(\text{Fe}-\text{C})$  in the adsorption complex is 2.16 Å. Comparison of the total energies of the adsorbed benzene oxide molecule and oxepin, adsorbed on the  $\pi$ -bond, indicates the possibility of equilibrium between these two structures. After the breaking of a C–O bond of the benzene oxide molecule, an adsorbed zwitterion is formed. One adsorbed structure could be identified. Adsorption occurs via the O atom, as in previous cluster model calculations. The bond distance  $R(\text{Fe}-\text{O}) = 1.80$  Å corresponds to a typical Fe–O bond. The optimized structure is shown in Figure 8. For both type of calculations (the periodic model and the cluster model), the intermediate is less stable than the adsorbed benzene oxide molecule (by 7 kcal/mol). This transformation is the rate-limiting step of the reaction. The formation of the keto-tautomer molecule is exothermic. This molecule adsorbs also via the O atom. The optimized structure of the keto-tautomer is shown in Figure 9. The transformation of the intermediate to the keto-tautomer is favorable by approximately –23 kcal/mol. The calculated transformation energy differs from that computed for the cluster model. For

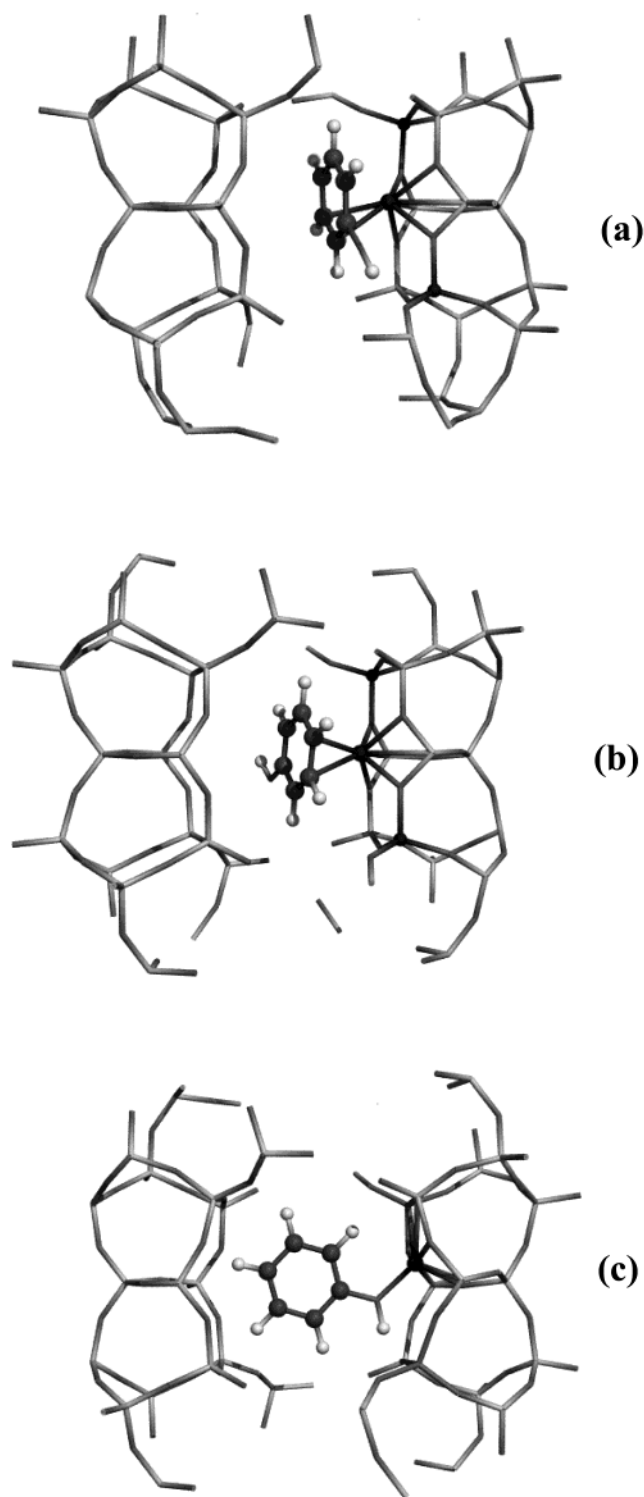


**Figure 10.** Adsorption complexes of the phenol molecule in the cavity of ferrierite.

cluster model calculations, it is  $-42$  kcal/mol.<sup>17</sup> There are also differences in the calculated structure of the adsorption complex. For periodic calculations, the C=O bond length is  $1.31$  Å and the Fe–O bond length is  $1.91$  Å in the adsorbed keto-tautomer molecule. For cluster calculations, these values are  $1.25$  and  $1.96$  Å, respectively.

The final product of the reaction is the phenol molecule. For the phenol molecule, we have found three adsorption complexes. Their structures are shown in Figure 10. In two cases, adsorption interaction occurs via the  $\pi$ -system, and in one case, the

interaction occurs via the O atom. The complex depicted in Figure 10a is the most stable. The structure of this adsorption complex completely differs from that for cluster model calculations. Adsorption occurs via the  $\pi$ -system; the two bond distances  $R(\text{Fe}–\text{C})$  are  $2.37$  and  $2.34$  Å, and the four distances  $R(\text{Fe}–\text{C})$  are  $\sim 2.55$  Å. The adsorption complex is additionally stabilized by the hydrogen bonding between the H atom of the hydroxyl group of the phenol molecule and the O atom of the zeolite lattice. This hydrogen bond is strong enough; the distance  $\text{OH}\cdots\text{O}_{\text{lattice}}$  is  $1.66$  Å. The second adsorption complex via the  $\pi$ -system (depicted in Figure 10b) differs from that in Figure 10a by lack of hydrogen bonding; other features of the adsorption structure in Figure 10b are the same as that for Figure 10a. The difference in stability of these complexes ( $9.3$  kcal/mol) is equal to the energy of the hydrogen bond. The energy of transformation from the adsorbed keto-tautomer to the adsorbed phenol molecule for the complex in Figure 10a is  $-33$  kcal/mol. In the case of cluster calculations, it is  $-4$  kcal/mol, with adsorption via the O atom.

Additional calculations have been performed to interpret the observed difference between these two approaches. Comparison of the adsorption structures for periodic and cluster model calculations indicates the strong effect of pore constraints. This effect is well-observed on the calculated structures of oxepin and phenol molecules. Arrangement of these molecules in the (*ab*) crystallographic plane is unfavorable. Because of repulsion with the zeolite lattice, molecules are situated in the (*bc*) plane. This results in different bonding, compared to the cluster model calculations, and, consequently, it influences the energetic profile of the reaction.

The next important question is related to the observed structural difference of the adsorption modes for the phenol molecule. Is the adsorption on the  $\pi$ -system a real mode, or is it an artifact of the computational method? To clarify the reason for disagreement between the cluster model and the periodic study, additional calculations of the adsorption complexes have been performed. First, the PAW method was used to localize the adsorption complex of phenol molecule via the O atom. A higher cutoff of  $400$  eV has been used for these calculations. The final optimized structure found is the adsorption complex via the  $\pi$ -system. The shortest bond distances ( $R(\text{Fe}–\text{C})$ ) are  $2.25$  and  $2.28$  Å. A distortion in the coordination of the Fe atom with lattice O atoms has been found. Iron is connected to three O atoms, with bond distances of  $2.07$ ,  $2.10$ , and  $2.18$  Å. We then tried to find an adsorption complex of the phenol molecule via the  $\pi$ -system using full-electron cluster model calculations, as in ref 17. A very weak complex adsorption energy of  $5.5$  kcal/mol has been found. The shortest bond distances ( $R(\text{Fe}–\text{C})$ ), in this case, are  $2.47$  and  $2.59$  Å. Recall that the adsorption energy of the phenol molecule on the O atom is  $24$  kcal/mol.<sup>17</sup> The calculations of the adsorption complex, which were performed with the PW91 functional, were the same as those in the periodic calculations. Results are similar to those obtained with the B3LYP functional. One can conclude that differences between the functionals cannot explain the differences in the structure of the adsorption complexes. To distinguish between the effect of pore constraints and effect of pseudopotential approximation, in combination with the plane-wave basis set, cluster model calculations were performed for the phenol molecule using the VASP program. The chosen cluster was similar to that in previous calculations; however, the phenol molecule has been arranged in the (*bc*) crystallographic plane. The PAW method and a cutoff of  $400$  eV has been used to locate the adsorption complex. The initial structure is shown in



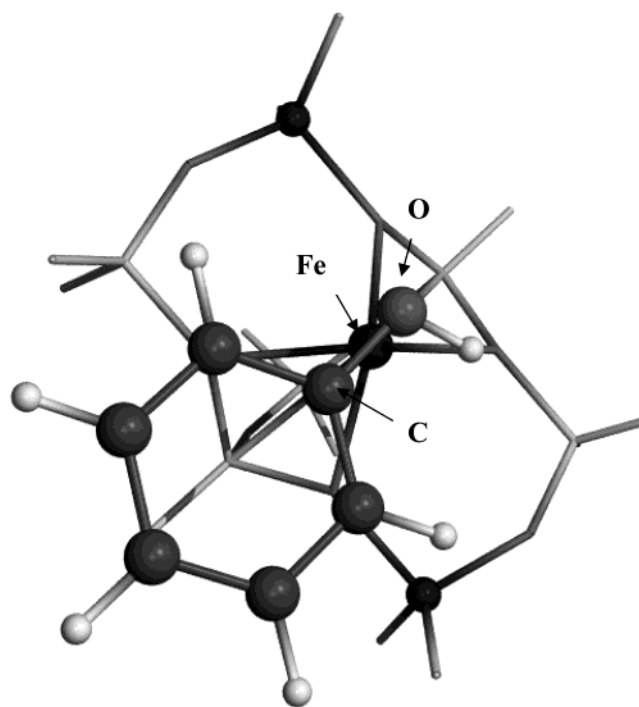


**Figure 11.** Initial structure of cluster model for periodic calculations. Distances  $R(\text{Fe}-\text{O}) = 1.73 \text{ \AA}$ .

Figure 11. In this structure, the atoms of the six-member ring and phenol molecule have been optimized. The size of the cluster is very large and, to avoid the interaction between unit cells, the double size of the unit cell in each direction was chosen. Initial results indicate that phenol adsorbs similarly on this cluster, as in the periodic system. These calculations lead to the conclusion that the observed differences between the periodic and cluster calculations might be an artifact of the pseudopotential with its standard restricted plane-wave basis. Specifically, a possible overestimation of the multicenter interactions of the Fe  $\alpha$ -site in the pseudopotential calculations leads to an artificial stabilization of the  $\pi$ -coordination of the Fe atom, relative to its O-atom coordination. The possibility of overestimation of multicenter interactions in pseudopotential calculations of transition-metal complexes has been demonstrated in ref 40.

## Conclusion

Periodic density functional theory (DFT) calculations have been performed for a model of the  $\alpha$ -oxygen active site present in zeolites with incorporated Fe ions. The model was constructed for  $\text{Fe}^{2+}$  ions that are located at the  $\alpha$ -cationic position of the ferrierite structure. The validity of the model then has been tested by calculating the bond energy for the  $\alpha$ -oxygen. It agrees well with the experimental value. The periodic calculations supported the important conclusion made in ref 17, that, in the oxidation steps, the transformation from benzene oxide to the zwitterion is the rate-limiting step. The adsorption modes found for the benzene oxide molecule and for the phenol in the periodic calculations differ from those for clusters. The use of pseudopotentials with its standard restricted plane wave basis is the most-probable reason for the differences that have been observed.

**Acknowledgment.** The Dutch Science Foundation is gratefully acknowledged for the financial support of the collaborative Russian–Dutch Project NOW-19-0411999. The authors also

thank Dr. Peter Vassilev and Dr. Xavier Rozanska for help with the calculations.

## References and Notes

- (1) Kharitonov, A. S.; Alexandrova, T. N.; Vostrikova, L. A.; Sobolev, V. L.; Ione, K. G.; Panov, G. I. USSR Patent No. 1 805 127, 1988.
- (2) Gubelmann, M. H.; Tirel, P. J. Fr. Patent No. 2 630 735, 1988.
- (3) Iwamoto, M.; Matsukami, K.; Kagawa, S. *J. Phys. Chem.* **1983**, *87*, 903.
- (4) Suzuki, E.; Makashiro, K.; Ono, Y. *Chem. Soc. Jpn. Chem. Commun.* **1988**, 953.
- (5) Ribera, A.; Arends, I. W. C. E.; de Vries, S.; Perez-Ramirez, J.; Sheldon, R. A. *J. Catal.* **2000**, *195*, 287.
- (6) Panov, G. I.; Kharitonov, A. S.; Fenelonov, V. B.; Voskresenskaya, T. P.; Rudina, N. A.; Molchanov, V. V.; Plyasova, L. M. *Zeolites* **1995**, *15*, 253.
- (7) Panov, G. I.; Kharitonov, A. S.; Sobolev, V. I. *Appl. Catal., A* **1993**, *98*, 1.
- (8) Sobolev, V. I.; Dubkov, K. A.; Paukshtis, E. A.; Pirutko, L. V.; Rodkin, M. A.; Kharitonov, A. S.; Panov, G. I. *Appl. Catal.* **1996**, *141*, 185.
- (9) Dubkov, K. A.; Ovanesyan, N. S.; Shteinman, A. A.; Starokon, E. V.; Panov, G. I. *J. Catal.* **2002**, *207*, 341.
- (10) Perez-Ramirez, J.; Kapteijn, F.; Mul, G.; Moulijn, A. *Catal. Commun.* **2002**, *3*, 19.
- (11) Kharitonov, A. S.; Panov, G. I.; Sheveleva, G. A.; Pirutko, L. V.; Voskresenskaya, T. P.; Sobolev, V. I. USSR Patent No. 2 074 164.
- (12) Bordiga, S.; Buzzoni, R.; Geobaldo, F.; Lamberti, C.; Giamello, E.; Zecchina, A.; Leofanti, G.; Petrini, G.; Tozzola, G.; Vlaic, G. *J. Catal.* **1996**, *158*, 486.
- (13) Ovanesyan, N. S.; Shteinman, A. A.; Sobolev, V. I.; Dubkov, K. A.; Panov, G. I. *Kinet. Katal.* **1998**, *39*, 863.
- (14) Panov, G. I. *CATTECH* **2000**, *4*, 18.
- (15) Dubkov, K. A.; Sobolev, V. I.; Talsi, E. P.; Rodkin, M. A.; Watkins, N. H.; Shteinman, A. A.; Panov, G. I. *J. Mol. Catal. A* **1997**, *123*, 155.
- (16) Yoshizawa, K.; Shiota, Y.; Yumura, T.; Yamabe, T. *J. Phys. Chem. B* **2000**, *104*, 734.
- (17) Kachurovskaya, N. A.; Zhidomirov, G. M.; Hensen, E. J. M.; van Santen, R. A. *Catal. Lett.* **2002**, *86*, 25.
- (18) Wichterlová, B.; Dědeček, J.; Sobalík, Z. Redox Catalysis over Molecular Sieves: Structure and Function of Active Sites. In *Proceedings of the 12th International Zeolite Conference*; Treacy, M. M. J., Marcus, B. K., Bisher, M. E., Higgins, J. B., Eds.; Materials Research Society: Warrendale, PA, 1999; Vol. 2, p 941.
- (19) Nováková, J.; Lhotka, M.; Tvarůžková, Z.; Sobalík, Z. *Catal. Lett.* **2002**, *83*, 215.
- (20) Kasperek, G. J.; Bruce, T. C.; Yagi, H.; Jerina, D. M. *J. Am. Chem. Soc.* **1973**, *95*, 6041.
- (21) Kasperek, G. J.; Bruce, T. C. *J. Am. Chem. Soc.* **1972**, *94*, 152.
- (22) van Santen, R. A.; Kramer, J. G. *Chem. Rev.* **1995**, *3*, 637.
- (23) Sinclair, P. E.; de Vries, A.; Sherwood, P.; Catlow, C. R. A.; van Santen, R. A. *J. Chem. Soc., Faraday Trans.* **1998**, *94*, 3401.
- (24) Shubin, A. A.; Yakovlev, A. L.; Zhidomirov, G. M.; van Santen, R. A. *J. Phys. Chem. B* **2001**, *105*, 4928.
- (25) Payne, M. C.; Teter, M. P.; Allan, D. C. *Rev. Mod. Phys.* **1992**, *64*, 1045.
- (26) Vanderbilt, D. *Phys. Rev. B* **1990**, *41*, 7892.
- (27) Allan, D. C.; Teter, M. P. *Phys. Rev. Lett.* **1987**, 1136.
- (28) Bar-Yam, Y.; Pantelides, S. T.; Joannopoulos, J. D. *Phys. Rev. B* **1989**, *39*, 3396.
- (29) Rappe, A. M.; Rabe, K. M.; Kaxiras, E.; Joannopoulos, J. D. *Phys. Rev. B* **1990**, *41*, 1227.
- (30) Trouillier, N.; Martins, J. L. *Phys. Rev. B* **1991**, *43*, 1993.
- (31) Barbosa, L. A. M. M.; van Santen, R. A. *J. Am. Chem. Soc.* **2001**, *123*, 4530.
- (32) (a) Kresse, G.; Hafner, J. *Phys. Rev. B* **1993**, *48*, 13115. (b) Kresse, G.; Hafner, J. *Phys. Rev. B* **1994**, *49*, 14251. (c) Kresse, G.; Furthmüller, J. *Comput. Mater. Sci.* **1996**, *6*, 15. (d) Kresse, G.; Furthmüller, J. *Phys. Rev. B* **1996**, *54*, 11169.
- (33) Perdew, J. P.; Burke, K.; Wang, Y. *Phys. Rev. B* **1996**, *54*, 16533.
- (34) Kresse, G.; Hafner, J. *J. Phys. Condens. Matter* **1994**, *6*, 8245.
- (35) Vos, A. N.; Rozanska, X.; Schoonheydt, R. A.; van Santen, R.; Hutschka, F.; Hafner, J. *J. Am. Chem. Soc.* **2001**, *123*, 2799.
- (36) Kresse, G.; Joubert, D. *Phys. Rev. B* **1999**, *59*, 1758.
- (37) Blöchl, P. E. *Phys. Rev. B* **1994**, *50*, 17953.
- (38) Panov, G. I.; Uriarte, A. K.; Rodkin, M. A.; Sobolev, V. I. *Catal. Today* **1998**, *41*, 365.
- (39) Choudhary, V. R.; Srinivasan, K. R. *Chem. Eng. Sci.* **1987**, *42*, 382.
- (40) Bagatur'yants, A. A.; Safonov, A. A.; Stoll, H.; Werner, H.-J. *J. Chem. Phys.* **1998**, *109*, 3096.